Co K-edge XANES of LiCoO2 and CoO2 with a variety of structures by supercell density functional calculations with a core hole

AUTHOR(S):

Koyama, Yukinori; Arai, Hajime; Ogumi, Zempachi; Tanaka, Isao; Uchimoto, Yoshiharu

CITATION:

Koyama, Yukinori ...[et al]. Co K-edge XANES of LiCoO2 and CoO2 with a variety of structures by supercell density functional calculations with a core hole. PHYSICAL REVIEW B 2012, 85(7): 075129.

ISSUE DATE:

2012-02

URL:

http://hdl.handle.net/2433/161779

PHYSICAL REVIEW B **85**, 075129 (2012)

Co *K*-edge XANES of $LiCoO_2$ and CoO_2 with a variety of structures by supercell density functional calculations with a core hole

Yukinori Koyama,* Hajime Arai, and Zempachi Ogumi
Office of Society-Academia Collaboration for Innovation, Kyoto University, Gokasho, Uji, Kyoto 611-0011, Japan

Isao Tanaka
Department of Materials Science and Engineering, Graduate School of Engineering, Kyoto University, Yoshida, Sakyo, Kyoto 606-8501, Japan

Yoshiharu Uchimoto
Graduate School of Human and Environment Studies, Kyoto University, Yoshida Nihon-matsu, Sakyo, Kyoto 606-8501, Japan
(Received 25 May 2011; published 27 February 2012)

Co *K*-edge x-ray absorption near edge structures (XANES) of $LiCoO_2$ and CoO_2 with a variety of structures, and their orientation dependence, have been evaluated by density functional theory calculations using supercells with a core hole. The spectrum of the layered rocksalt $LiCoO_2$, which is available by experiment, is well reproduced. The effects of the stacking sequence of layered structures and those of Li/Co arrangement in ordered rocksalt polymorphs on XANES are systematically investigated. The spectral shape is sensitive to the stacking sequence in the layered $LiCoO_2$ polymorphs, while it is insensitive in the corresponding CoO_2. On the other hand, the ordered-rocksalt polymorphs of $LiCoO_2$ with different Li/Co arrangements exhibit similar spectra, while strong dependence on the manner of the ordering is found in CoO_2. Although XANES is rich in information, the use of theoretical fingerprints is desirable for reliable analysis of the oxidation states and identification of the stacking sequence and the manner of ordering.

DOI: 10.1103/PhysRevB.85.075129 PACS number(s): 78.70.Dm, 61.05.cj

I. INTRODUCTION

Lithium-ion batteries are one of the most promising systems for powering hybrid/pure electric vehicles and for storage of renewable energy. While lithium-ion batteries are widely used today as electric power sources for portable devices, further development is necessary for large-scale applications, especially to achieve longer life and higher safety. The key to this goal is a better understanding of reactions in charging, discharging, and storage processes.[1–3] Among various techniques, the spectroscopic method for measuring x-ray absorption near edge structures (XANES) is very powerful because of the specificity to elements and sensitivity to the electronic states and local geometry of the exited atoms. Moreover, high intensity x-ray sources from synchrotron radiation centers enable us to measure XANES at transition-metal (*TM*) *K* edges *in situ*,[4,5] providing rich information on the electronic states and local geometry of positive electrodes of the lithium-ion batteries.

XANES has been empirically interpreted simply by comparison with experimental spectra of reference phases (*experimental fingerprints*). The fingerprinting technique can be used to characterize polymorphs.[6–8] Sometimes, qualitative analysis of the oxidation states of the *TM* species is made from energy shifts of peaks. The fingerprinting technique, however, has obvious limitations for observing novel or exotic compounds, surfaces, and interfaces, because no experimental spectra are available as references. Computational techniques that are capable of predicting reliable theoretical spectra (*theoretical fingerprints*) are therefore very useful. In general, XANES corresponds to the electronic transition from core orbitals of the selected atoms to unoccupied bands following the electric dipole selection rule. For instance, *TM*-*K* XANES corresponds to the transition from *TM*-1*s* core orbitals to *TM*-4*p* states, and *TM*-$L_{2,3}$ XANES corresponds to that from *TM*-2*p* to *TM*-3*d*. To study theoretical *TM*-*K* XANES, two approaches have been widely used. One is density functional theory (DFT) calculation using supercells with a core hole,[9–12] and the other is the multiple-scattering method.[13,14] For *TM*-$L_{2,3}$ XANES, other approaches are required because a strong correlation among the *TM*-3*d* electrons and the 2*p* core hole causes widely spread multiplet structures. In our group, *TM*-$L_{2,3}$-edge XANES has been discussed using the *ab initio* configuration-interaction approach.[15]

Despite that the supercell DFT calculation with the core hole and the multiple-scattering method can successfully evaluate reliable *TM* *K*-edge XANES, theoretical XANES of the electrode materials of the lithium-ion batteries are limited.[16–18] A pseudopotential calculation with the generalized gradient approximation and the Hubbard model correction (GGA + *U*) was reported for $LiCoO_2$ with special interest in the angular dependence of core hole screening.[18] They reported that the pre-edge features of the spectrum were dependent on the exchange-correlation term for the strongly correlated Co-3*d* electrons. But the effects of the oxidation states and the crystal structure on XANES have not been revealed yet. In the present work, Co *K*-edge XANES are systematically evaluated for polymorphs of $LiCoO_2$ and Li-removed CoO_2 using the supercell DFT calculations to discuss the effects of the Li removal and the crystal structure on XANES.

II. CALCULATION METHOD

A. Crystal structures

The stable phase of $LiCoO_2$ under the ordinary condition is isostructural with α-$NaFeO_2$, in which oxygen ions form

a cubic close-packed sublattice, and Li and Co ions occupy octahedral interstitial sites of alternate (111) layers. This structure is an ordered rocksalt type of a layered form with a rhombohedral symmetry. The stacking sequence of the layered rocksalt was named O3.[19] Several polymorphs of $LiCoO_2$ have been reported. A cubic phase has been synthesized at a low temperature of about 400 °C.[20,21] This phase is called LT-$LiCoO_2$. A spinel-related model is proposed for this structure, in which Li ions occupy the octahedral 16*c* site instead of the tetrahedral 8*a* site.[21,22] Layered polymorphs with O2 and O4 stacking sequences (O2-$LiCoO_2$ and O4-$LiCoO_2$, respectively) have been synthesized by a Na^+/Li^+ ion-exchange technique from P2-Na_xCoO_2 ($x \sim 0.7$)[23–25] and OP4-$Li_xNa_yCoO_2$ ($x \sim 0.4$, $y \sim 0.4$).[26,27] In addition, some other ordered rocksalt structures are known for lithium *TM* oxides of $LiTMO_2$, namely γ-$LiFeO_2$ and $LiMnO_2$.[28,29]

In the present work, seven sets of $LiCoO_2$ and CoO_2, including above-mentioned polymorphs, are examined. The sets are the O3-type layered rocksalt, three kinds of layered structures with the stacking sequences of O1, O2, and O4, and three kinds of ordered rocksalt of the spinel-related type, zigzag-layered type (which is isostructural with $LiMnO_2$), and γ-$LiFeO_2$ type. The O1-type layered structure has not been reported yet for lithium *TM* oxides, while some chalcogenides, such as $LiTMS_2$ (*TM* = Ti, V, and Cr), form this structure. Since some of the polymorphs have not yet been synthesized, the crystallographic parameters of all the polymorphs were evaluated by the DFT calculations in the present study. CoO_2 polymorphs were constructed simply by removal of the Li ions and structural optimization under the given symmetries.

The DFT calculations were performed using the plane-wave basis projected-augmented-wave (PAW) method implemented in the VASP code.[30–32] Exchange-correlation interaction was treated by a hybrid functional based on a screened Coulomb potential formulated by Heyd, Scuseria, and Ernzerhof (HSE06).[33] Spin polarization was considered with ferromagnetic ordering for simplicity. Radii of the PAW potentials used were 1.38, 1.30, and 0.82 Å for Li, Co, and O, respectively. Li-1*s*, Co-1*s* to 3*p*, and O-1*s* orbitals were treated as the core. The plane-wave basis set was determined by a cutoff energy of 500 eV. The integral in the reciprocal space was made by the Gaussian smearing technique with $\sigma = 0.1$ eV. Atomic positions and lattice constants were relaxed until residual forces and stresses became typically less than 0.01 eV/Å and 0.1 GPa, respectively. The calculated lattice constants agreed well with the experimental ones, with an error of 0.5% or less for the reported $LiCoO_2$ polymorphs.

B. XANES spectra

Co *K*-edge XANES of the $LiCoO_2$ and CoO_2 polymorphs were evaluated by DFT calculations using the supercells. All-electron full-potential augmented-plain-wave (APW) plus local-orbital method implemented in the WIEN2K package[34,35] was used. The hybrid exchange-correlation functional is prohibitive for large supercells with a number of unoccupied bands. The present work focuses on the main peaks of Co-*K* XANES that are expected to not be greatly affected by the strong correlation among the Co-3*d* electrons. Therefore, the GGA formulated by Perdew, Burke, and Ernzerhof (PBE)[36] was used for the exchange-correlation interaction. The spin polarization was considered with the ferromagnetic ordering. Atomic sphere radii used were 0.85 Å for all Li, Co, and O. Co-1*s*, 2*s*, 2*p*, and O-1*s* orbitals were treated as the core. The basis set of the APW was determined by a cutoff energy of 260 eV ($R_{\mathrm{MT}} \times K_{\max} = 7.0$). The supercells were constructed by expansion of the unit cells so that they contained about 100–200 atoms, and the lattice constants were about 10 Å or more. Single core holes were introduced into the Co-1*s* core orbitals with specific spin states for the excited states. The reciprocal-space integral was made by the tetrahedron method typically using a $4 \times 4 \times 4$ mesh. The theoretical spectra were calculated for the electric dipole transition as

$$\mu(E, \boldsymbol{e}) \propto \sum_f |\langle \phi_f | \boldsymbol{e} \cdot \boldsymbol{r} | \phi_i \rangle|^2 \delta(E + E_i - E_f), \qquad (1)$$

where E, E_i, and E_f are photon energy, total energy of the initial state, and total energy of the final state, respectively. ϕ_i and ϕ_f are one-electron wave functions of the core orbital and the excited electron, respectively. $\boldsymbol{e}$ and $\boldsymbol{r}$ are the unit vector for the polarization direction of the x-ray and the position vector, respectively. Orientationally averaged spectra were calculated as

$$\mu = \tfrac{1}{3}[\mu(\boldsymbol{e} \parallel \boldsymbol{x}) + \mu(\boldsymbol{e} \parallel \boldsymbol{y}) + \mu(\boldsymbol{e} \parallel \boldsymbol{z})]. \qquad (2)$$

The spectra were broadened both by a Lorentzian function (a full-width at half-maximum (FWHM) of 1.4 eV) as the lifetime of the core orbitals[37] and by a Gaussian function (a FWHM of 1.5 eV) for resolution of spectrometers. The FWHM of 1.5 eV corresponds to an energy resolution, $\Delta E/E$, of 2×10^{-4} at Co *K*-edge, which is typical for Si(111) monochromaters.

III. RESULTS AND DISCUSSIONS

A. Co-*K* XANES of layered rocksalt $LiCoO_2$

Figure 1 shows calculated and experimental Co-*K* XANES of the layered-rocksalt $LiCoO_2$. The calculation successfully reproduced the major peaks and shoulders (*B*–*E* in the figure) of the experimental XANES except for the pre-edge peak *A*, with respect to not only relative energy but also absolute transition energy. The error of the absolute transition energy was less than 1 eV in the layered-rocksalt $LiCoO_2$. A similar core-hole supercell calculation was reported in Ref. 18, but they matched the transition energy to the experiment. The transition energy of the present study was obtained by the difference of the total energies at the final and initial states, as shown in Eq. (1). The agreement of the absolute transition energy is quite satisfactory, although a relatively large error of the transition energy for the pre-edge peak *A* can be seen, which can be ascribed to the imperfection of the exchange-correlation term for the strongly correlated Co-3*d* electrons in the present study. It should be noted that the spin state of the core hole is essential to obtain the transition energy. If the spin state of the core hole is not correctly treated, the error of the transition energy is much larger. For example, when a half of the hole was introduced to each of spin-up and spin-down states, the excited state became higher in energy by about 30 eV in the case of the layered-rocksalt $LiCoO_2$, resulting in a higher transition energy by 30 eV.

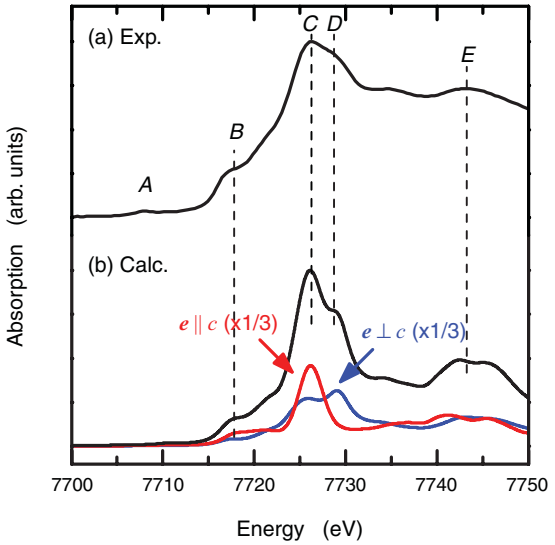

FIG. 1. (Color online) Co-K XANES of layered-rocksalt $LiCoO_2$ by (a) experiment and (b) DFT calculation. Orientation-dependent spectra are also shown for the calculation.

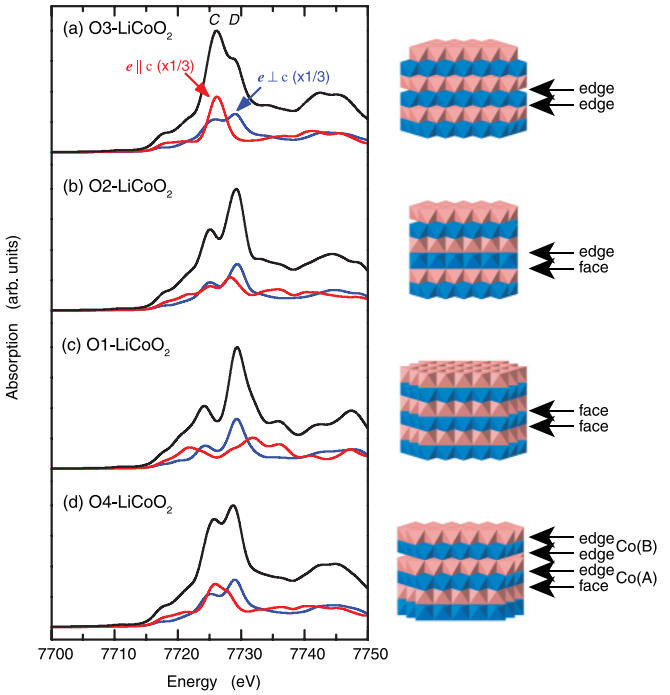

FIG. 2. (Color online) Calculated Co-K XANES of layered $LiCoO_2$ with the stacking sequence of (a) O3, (b) O2, (c) O1, and (d) O4 types with their orientation dependence. Schematic images of the corresponding stacking sequences are also shown. Blue and red polyhedra denote CoO_6 and LiO_6 octahedra, respectively.

Since the layered rocksalt is not a cubic system, orientation dependence of XANES can be expected. The orientation-dependent XANES can be measured by polarized x rays in which the electric field $\boldsymbol{e}$ is either parallel to the c axis ($\boldsymbol{e} \parallel c$) or perpendicular to the c axis ($\boldsymbol{e} \perp c$). The average of the two spectra corresponds to that obtained from a polycrystalline sample. The calculated orientation-dependent spectra for ($\boldsymbol{e} \parallel c$) and ($\boldsymbol{e} \perp c$) are also illustrated in Fig. 1. A clear difference between the two spectra can be seen for the major peak at 7720–7730 eV. The ($\boldsymbol{e} \parallel c$) spectrum consists of a single peak, while the ($\boldsymbol{e} \perp c$) one has double peaks. Peak C is, therefore, composed of both ($\boldsymbol{e} \parallel c$) and ($\boldsymbol{e} \perp c$) components, while peak D is composed of only the ($\boldsymbol{e} \perp c$) one. The different spectral shapes of the two orientations are similar to those reported in Ref. 18. If the structure is the cubic rocksalt type, the orientation dependence should disappear. The differences between the two orientation-dependent spectra are caused by the different species of Li and Co and trigonal distortion along the c axis (84° of O-Co-O angle). Therefore, changes in XANES can be expected by the different stacking sequence and Li/Co arrangement. This will be discussed in the following sections.

B. Co-K XANES of layered polymorphs

Layered polymorphs of $LiCoO_2$ with different stacking sequences have been reported. In the present study, the polymorphs of O1, O2, and O4 stacking sequences were examined, as well as the O3 type. The structures of the layered polymorphs are schematically shown in Fig. 2. In the O3-type layered-rocksalt $LiCoO_2$, CoO_6 octahedra share only edges with LiO_6 ones. In O1-$LiCoO_2$, the oxygen ions form a hexagonal close-packed sublattice, and the CoO_6 octahedra share two faces with the LiO_6. In the O2 type, the CoO_6 share a single face with the LiO_6. In the O4 type, there are two kinds of Co layers. One layer has a similar local geometry to O2-$LiCoO_2$ and the CoO_6 octahedra share a single face with the LiO_6, while the CoO_6 of the other layer share only the edges as in O3-$LiCoO_2$. These two Co sites will be called Co(A) and Co(B), respectively, according to the corresponding Wyckoff letters. The calculated lattice constants and the distance between Co layers of the four layered polymorphs are summarized in Table I. Comparing the lattice constants and Co-Co interlayer distances, the expansion of the interlayer distance and slight reduction of the a axis can be seen as the sharing manner changes from the edge to the face. The larger interlayer distance for the face sharing can be ascribed to the stronger electrostatic repulsion between the Co and Li ions. The stronger repulsion enhances the trigonal distortion to keep Co-O bond length constant. O4-$LiCoO_2$ has two kinds of interlayer distances, with and without the face-shared pair of the Co and Li layers. With the face-shared pair, the Co-Co interlayer distance is 4.76 Å and the same as that of

TABLE I. Lattice constants and Co-Co interlayer distances of layered $LiCoO_2$ polymorphs.

Stacking sequence	a (Å)	c (Å)	Interlayer distance (Å)
O3	2.802	14.05	4.68
O2	2.791	9.51	4.76
O1	2.778	4.84	4.84
O4	2.798	18.90	4.69, 4.76

TABLE II. Interatomic distances of Co-O, Co-Co and Co-Li in layered $LiCoO_2$ polymorphs.

Stacking sequence	Co-O (Å)	Co-Co (Å)	Co-Li (Å)
O3	1.91 × 6	2.80 × 6	2.85 × 6
O2	1.91 × 6	2.79 × 6	2.45 × 1, 2.82 × 3
O1	1.91 × 6	2.78 × 6	2.42 × 2
O4; Co(A)	1.91 × 6	2.80 × 6	2.44 × 1, 2.83 × 3
O4; Co(B)	1.91 × 6	2.80 × 6	2.83 × 3, 2.86 × 3

O2-$LiCoO_2$, while the distance without the face-shared pair is 4.69 Å and the same as that of O3-$LiCoO_2$. Table II summarizes the calculated Co-O, Co-Co, and Co-Li distances in the four layered polymorphs. Co-O bond lengths are almost constant among the four layered polymorphs. The Co-Co distances, which are identical to the a axis, do not change so much. The CoO_2 slabs, therefore, have very similar geometry among the four layered $LiCoO_2$ polymorphs. In contrast, the different stacking sequence causes the difference in the sharing manner of the CoO_6 and LiO_6 octahedra and different Co-Li distances: the face-shared distances are 2.42–2.45 Å, while the edge-shared ones are 2.83–2.86 Å.

Calculated XANES of the layered polymorphs of $LiCoO_2$ are illustrated in Fig. 2 with their orientation dependence. The shapes of the main peaks clearly differ among the layered polymorphs. At a glance, the strongest peak C of O3-$LiCoO_2$ becomes weaker and peak D becomes stronger as the fraction of the face-shared CoO_6 and LiO_6 octahedra increases. The cause of the difference can be understood by the orientation-dependent spectra.

In O3-$LiCoO_2$, the ($\boldsymbol{e} \parallel c$) spectrum is a singlet and the ($\boldsymbol{e} \perp c$) is a doublet, as described above. Peak C is composed of both the ($\boldsymbol{e} \parallel c$) and ($\boldsymbol{e} \perp c$) spectra, while peak D is composed of only the ($\boldsymbol{e} \perp c$) one. The other layered polymorphs also exhibit similar ($\boldsymbol{e} \perp c$) spectra with double peaks. This suggests similar electronic states in the CoO_2 slabs among the four layered polymorphs due to the similar geometry. In contrast, the ($\boldsymbol{e} \parallel c$) spectra exhibit remarkable differences. The O2 type exhibits a broad peak, and the O1 type has broader double peaks. This suggests that the electronic states perpendicular to the layers are strongly affected by the sharing manner of the CoO_6 and LiO_6 octahedra and by the Co-Li distances. The broadening of the ($\boldsymbol{e} \parallel c$) spectrum makes the averaged spectrum similar to the ($\boldsymbol{e} \perp c$) component and the strongest peak change from C to D.

O4-$LiCoO_2$ has the two Co sites. XANES of O4-$LiCoO_2$ is, therefore, superposition of the spectra from the two Co sites. Although the spectra from the two sites are hardly separated in experiments, the theoretical calculation can provide individual spectra. Figure 3 illustrates Co-K XANES from the Co(A) and Co(B) sites of O4-$LiCoO_2$. It is clear that the spectrum from the Co(A) site is similar to that of O2-$LiCoO_2$, and that from the Co(B) is similar to that of O3-$LiCoO_2$. The total spectrum of O4-$LiCoO_2$ is, therefore, close to an average of those of O3-$LiCoO_2$ and O2-$LiCoO_2$. The close similarity has been also pointed out by experiments.[38] This is natural, since the local structure and electronic states of the Co(A) and

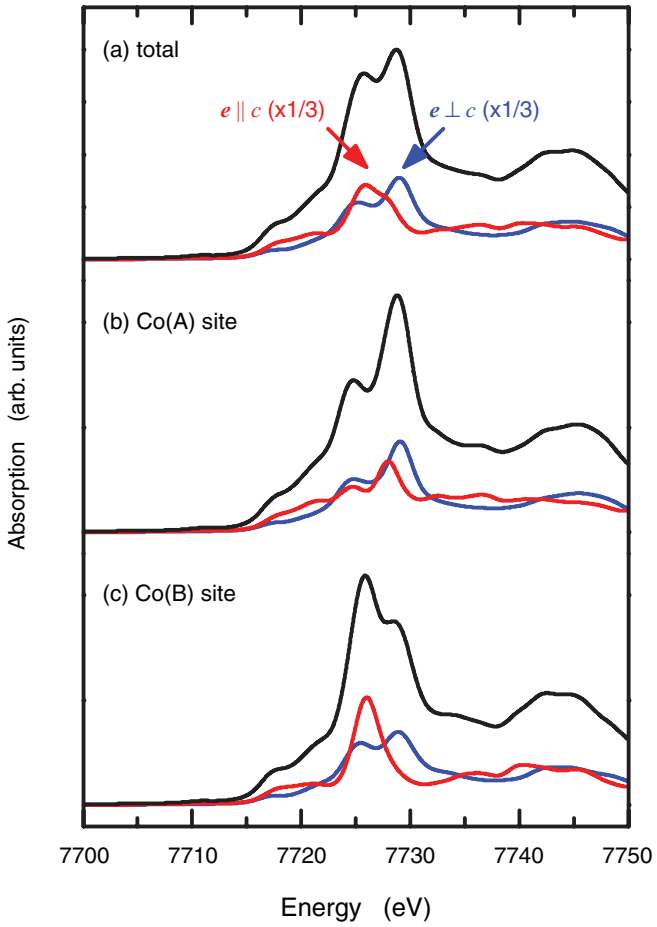

FIG. 3. (Color online) Calculated Co-K XANES of (a) total, (b) Co(A) site, and (c) Co(B) site of O4-$LiCoO_2$ with their orientation dependence.

Co(B) sites are respectively similar to those of O2-$LiCoO_2$ and O3-$LiCoO_2$.

As mentioned above, the difference in XANES among the layered $LiCoO_2$ polymorphs is caused by the different sharing manner of the CoO_6 and LiO_6 octahedra. It is interesting to know whether the spectra differ even without Li ions. Figure 4 illustrates calculated Co-K XANES of the layered CoO_2 polymorphs with the four stacking sequences. It is clear that the difference among the four CoO_2 polymorphs becomes much smaller. The orientation-dependent spectra show that the lower-energy peaks of the double peaks of the ($\boldsymbol{e} \perp c$) spectra become weak by the Li removal. The ($\boldsymbol{e} \parallel c$) spectra become broader for all the four polymorphs. Thus, the four polymorphs exhibit similar spectra. Comparing XANES between $LiCoO_2$ and CoO_2, the energy shift of the main peak looks significant for the O3 type, while the shifts for the O2 and O1 types are small. This is because the ($\boldsymbol{e} \parallel c$) spectrum becomes broader by the Li removal and peak D becomes the strongest over peak C for the O3 type. This causes the large apparent shift. In contrast, the main peaks of the O2 and O1 types are composed of the ($\boldsymbol{e} \perp c$) spectra for both $LiCoO_2$ and CoO_2. The apparent shift is, therefore, smaller than that of the O3 type. These differences in XANES by the Li removal can be discussed only when the *theoretical fingerprints* are available.

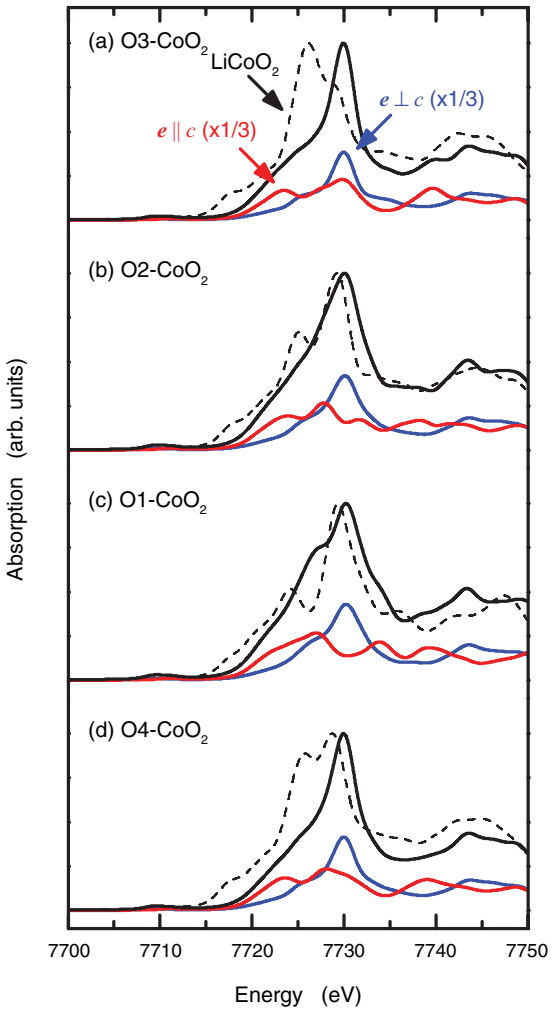

FIG. 4. (Color online) Calculated Co-K XANES of layered CoO_2 of (a) O3, (b) O2, (c) O1, and (d) O4 types, with their orientation dependence. Broken lines show XANES of $LiCoO_2$ with the same stacking sequence as eye guides.

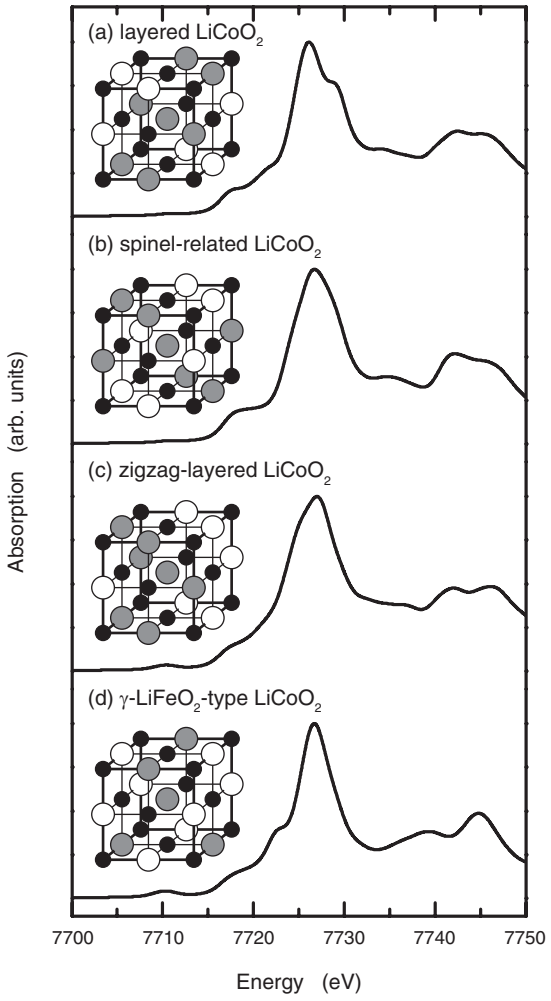

FIG. 5. Calculated Co-K XANES of ordered rocksalt $LiCoO_2$ polymorphs of (a) O3-type layered rocksalt, (b) spinel-related type, (c) zigzag-layered type, and (d) γ-$LiFeO_2$ type. Schematic images of the corresponding Li/Co arrangements are also shown. Open, grayed, and small black spheres denote Li, Co, and O ions, respectively.

C. Co-K XANES of ordered rocksalt polymorphs

Four kinds of ordered rocksalt polymorphs were examined in the present study to investigate the effects of Li/Co arrangements on XANES. They are the O3-type layered form, the spinel-related type, the zigzag-layered type, and the γ-$LiFeO_2$ type. They are known as ordered structures of lithium *TM* oxides: For instance, the layered structure for V, Cr, Co, and Ni, the spinel-related type for Ti, V, and Mn, the zigzag-layered type for Mn, and the γ-$LiFeO_2$ type for Sc and Fe are known to exist. The *fingerprints* of these polymorphs provide invaluable information not only to distinguish the manner of the ordering of samples, but also to investigate the magnitude of the disordering of the Li and Co ions introduced during the charge-discharge cycles and the long-term storage at high temperatures. The interatomic distances of the later three ordered-rocksalt polymorphs are summarized in Table III. The Co-O and Co-Co distances are almost constant among the four ordered rocksalt $LiCoO_2$, while the Co-Li ones are rather scattered.

TABLE III. Interatomic distances of Co-O, Co-Co and Co-Li in ordered-rocksalt polymorphs of $LiCoO_2$. See also Table II for O3-type layered rocksalt.

Ordering	Co-O (Å)	Co-Co (Å)	Co-Li (Å)
Spinel-related	1.91 × 6	2.82 × 6	2.82 × 6
Zigzag-layered	1.89 × 2, 1.93 × 4	2.81 × 2, 2.85 × 4	2.73 × 1, 2.88 × 4, 3.21 × 1
γ-$LiFeO_2$	1.90 × 2, 1.94 × 4	2.85 × 4	2.73 × 4, 2.85 × 4

Figure 5 illustrates the calculated XANES of the four ordered-rocksalt polymorphs of $LiCoO_2$ with the schematic images of the Li/Co arrangements. These four polymorphs exhibit similar XANES. This suggests that the exchange of cation species does not have a significant impact on the band structure of the unoccupied states as long as the overall cation ratio is unchanged. Despite the insensibility of XANES on the Li/Co arrangement, minor differences can be seen at the shoulder of the main peak (*D* in Fig. 1). The layered rocksalt exhibits the shoulder at the higher-energy side. The spinel-related polymorph has the broad main peak, and such a shoulder is unclear. The zigzag-layered one has a shoulder on the lower-energy side. The γ-$LiFeO_2$ type exhibits a sharp main peak. Therefore, precise XANES measurements may enable us to detect the difference in the Li/Co arrangement.

In sharp contrast to the $LiCoO_2$ polymorphs, Co-*K* XANES of Li-removed CoO_2 of the ordered-rocksalt polymorphs exhibit a remarkable dependence on the manner of the ordering, as shown in Fig. 6. In the spinel-related polymorph, both the top and foot of the main peak shift toward the higher-energy side by Li removal, which is similar to the O3-type layered rocksalt. On the other hand, in the zigzag-layered and γ-$LiFeO_2$-type polymorphs, the main peak broadens remarkably with a smaller energy shift of the peak top.

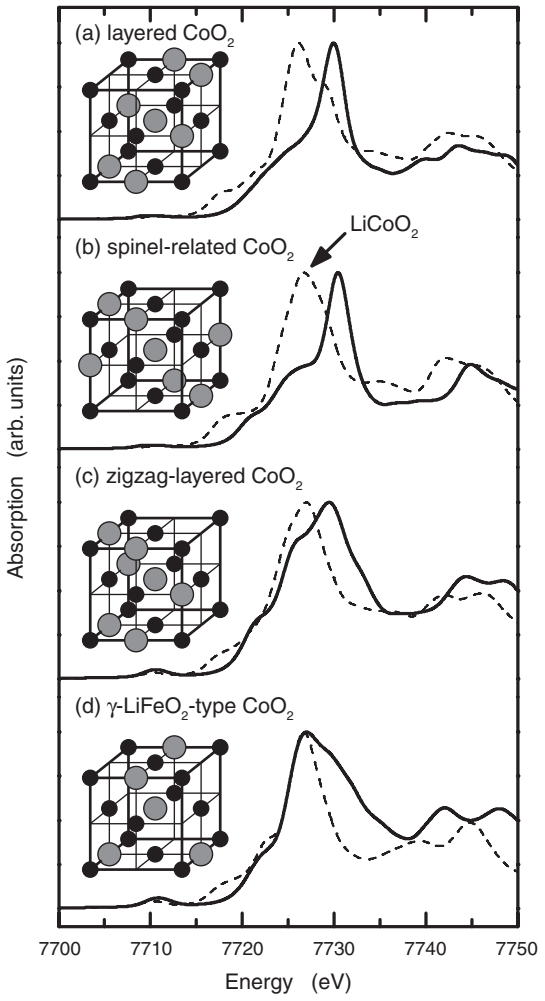

FIG. 6. Calculated Co-*K* XANES of ordered-rocksalt CoO_2 polymorphs of (a) layered rocksalt, (b) spinel-related type, (c) zigzag-layered type, and (d) γ-$LiFeO_2$ type. Broken lines show XANES of $LiCoO_2$ with the same Co arrangement as eye guides. Schematic images of the corresponding Co arrangements are also shown. Grayed and small black spheres denote Co and O ions, respectively.

Some readers might be puzzled by the different behaviors between the layered polymorphs and ordered-rocksalt ones associated with Li removal. However, the behaviors can be well explained by inspection of the difference in their atomic arrangements. Since the first (Co-O) coordination shells of Co ions are the same (sixfold coordinated) in all the $LiCoO_2$ and CoO_2 polymorphs, let us focus on the second (Co-Co and Co-Li) shells in the polymorphs. Among the layered $LiCoO_2$ polymorphs, the cation coordination number varies from 8 to 12. However, the coordination number becomes 6 after the Li removal, and the CoO_2 slabs have very similar geometry. This is the reason why the XANES spectra are different among the layered $LiCoO_2$ polymorphs and similar after the Li removal. On the other hand, among the ordered-rocksalt $LiCoO_2$ polymorphs, the coordination number is always 12. After the Li removal, it becomes 4 for the γ-$LiFeO_2$-type and 6 for the other three. In addition, the later three polymorphs have different Co arrangements, as schematically shown in Fig. 6. This causes the similar XANES spectra for $LiCoO_2$ and different ones for CoO_2.

Although the shape of the main peak changes remarkably with the manner of the ordering, the onset energy of the main peak is located commonly at around 7720 eV for CoO_2 and 7715 eV for $LiCoO_2$. Careful experimental inspection of the onset energy can be used to determine the oxidation states. However, the peak-top energy cannot be directly used as the measure of the oxidation states. The use of the *theoretical fingerprints* would be necessary for reliable analysis of the oxidation states and structures with varying stacking sequence and manner of ordering.

IV. CONCLUSIONS

Co-*K* XANES of $LiCoO_2$ and CoO_2 with a variety of structures, and their orientation dependence, have been evaluated by DFT calculations using the supercells with the core hole. The effects of the stacking sequence of the layered structures and those of the Li/Co arrangement in the ordered-rocksalt polymorphs on XANES have been systematically investigated. The experimental spectrum of the layered rocksalt $LiCoO_2$ was well reproduced. The error of the absolute transition energy was less than 1 eV by introduction of the core hole in the proper spin states.

The orientation-dependent spectra of the layered $LiCoO_2$ polymorphs showed the different ($\boldsymbol{e} \parallel c$) components and the similar ($\boldsymbol{e} \perp c$) ones among the different stacking sequences. This resulted in the sensitivity of the spectral shape of the orientationally averaged XANES to the stacking sequence in the layered $LiCoO_2$ polymorphs. On the other hand, Co-*K* XANES of the corresponding CoO_2 polymorphs was insensitive to the stacking sequence. Thus the apparent peak shift by the Li removal was strongly dependent on the stacking sequence.

The ordered-rocksalt polymorphs of $LiCoO_2$ with the different Li/Co arrangements exhibited similar spectra,

suggesting little effect of the exchange of the cation species on the band structure of the unoccupied states as long as the overall cation ratio is unchanged. In sharp contrast, the strong dependence of the spectral shape on the manner of the Li/Co arrangements was found in the corresponding CoO_2 polymorphs.

Although XANES is rich in information, the energies of the peaks and shoulders are strongly dependent on the structure even with the same chemical formula and the same oxidation state, as shown in Figs. 2 and 6. The *experimental fingerprints* require much attention be paid. The use of the *theoretical fingerprints* is desirable for reliable analysis of the oxidation states and identification of the stacking sequence and the manner of ordering.

ACKNOWLEDGMENTS

This work was supported by the Research and Development Initiative for Scientific Innovation of New Generation Battery (RISING) project from the New Energy and Industrial Technology Development Organization (NEDO).

*koyama@saci.kyoto-u.ac.jp

[1] B. Scrosati and J. Garche, J. Power Sources **195**, 2419 (2010).
[2] J. B. Goodenough and Y. Kim, Chem. Mater. **22**, 587 (2010).
[3] J.-M. Tarascon, Phil. Trans. R. Soc. A **368**, 3227 (2010).
[4] I. Nakai, K. Takahashi, Y. Shiraishi, and T. Nakagome, J. Physique IV**7**, 1243 (1997).
[5] J. McBreen and M. Balasubramanian, J. Miner. Met. Mater. Soc. **54**, 25 (2002).
[6] Y. Lee, H. Lim, S.-J. Kim, W.-J. Lee, and D.-H. Cho, Res. Chem. Intermed. **29**, 783 (2003).
[7] L. Bertini, P. Ghigna, M. Scavini, and F. Cargnoni, Phys. Chem. Chem. Phys. **5**, 1451 (2003).
[8] D. de Ligny, D. R. Neuville, L. Cormier, J. Roux, G. S. Henderson, G. Panczer, S. Shoval, A.-M. Flank, and P. Lagarde, J. Non-Crystalline Solids **355**, 1099 (2009).
[9] I. Tanaka, T. Mizoguchi, and T. Yamamoto, J. Am. Ceram. Soc. **88**, 2013 (2005).
[10] I. Tanaka and T. Mizoguchi, J. Phys. Condens. Matter **21**, 104201 (2009).
[11] W.-Y. Ching and P. Rulis, J. Phys. Condens. Matter. **21**, 104202 (2009).
[12] T. Mizoguchi, I. Tanaka, S.-P. Gao, and C. J. Pickard, J. Phys. Condens. Matter. **21**, 104204 (2009).
[13] A. Filipponi, A. DiCicco, and C. R. Natoli, Phys. Rev. B **52**, 15122 (1995).
[14] J. J. Rehr and R. C. Albers, Rev. Mod. Phys. **72**, 621 (2000).
[15] H. Ikeno, T. Mizoguchi, Y. Koyama, Z. Ogumi, Y. Uchimoto, and I. Tanaka, J. Phys. Chem. C **115**, 11871 (2011).
[16] J. Shirakawa, M. Nakayama, Y. Uchimoto, and M. Wakihara, Electrochem. Solid State Lett. **9**, A200 (2006).
[17] K. Tatsumi, Y. Sasano, S. Muto, T. Yoshida, T. Sasaki, K. Horibuchi, Y. Takeuchi, and Y. Ukyo, Phys. Rev. B **78**, 045108 (2008).
[18] A. Juhin, F. de Groot, G. Vankó, M. Calandra, and C. Brouder, Phys. Rev. B **81**, 115115 (2010).
[19] C. Delmas, C. Fouassier, and P. Hagenmuller, Physica B **99**, 81 (1980).
[20] R. J. Gummow, M. M. Thackeray, W. I. F. David, and S. Hull, Mater. Res. Bull. **27**, 327 (1992).
[21] M. Antaya, J. R. Dahn, J. S. Preston, E. Rossen, and J. N. Reimers, J. Electrochem. Soc. **140**, 575 (1993).
[22] R. J. Gummow, D. C. Liles, M. M. Thackeray, and W. I. F. David, Mater. Res. Bull. **28**, 1177 (1993).
[23] C. Delmas, J.-J. Braconnier, and P. Hagenmuller, Mater. Res. Bull. **17**, 117 (1982).
[24] J. M. Paulsen, J. R. Mueller-Neuhaus, and J. R. Dahn, J. Electrochem. Soc. **147**, 508 (2000).
[25] D. Carlier, I. Saadoune, L. Croguennec, M. Ménétrier, E. Suard, and C. Delmas, Solid State Ionics **144**, 263 (2001).
[26] S. Komaba, N. Yabuuchi, and Y. Kawamoto, Chem. Lett. **38**, 954 (2009).
[27] R. Berthelot, D. Carlier, M. Pollet, J.-P. Doumerc, and C. Delmas, Electrochem. Solid State Lett. **12**, A207 (2009).
[28] G. C. Mather, C. Dussarrat, J. Etourneau, and A. R. West, J. Mater. Chem. **10**, 2219 (2000).
[29] M. Wang and A. Navrotsky, J. Solid State Chem. **178**, 1230 (2005).
[30] G. Kresse and J. Furthmüller, Phys. Rev. B **54**, 11169 (1996).
[31] P. E. Blöchl, Phys. Rev. B **50**, 17953 (1994).
[32] G. Kresse and D. Joubert, Phys. Rev. B **59**, 1758 (1999).
[33] J. Heyd, G. E. Scuseria, and M. Ernzerhof, J. Chem. Phys. **124**, 219906 (2006).
[34] P. Blaha, K. Schwarz, G. K. H. Madsen, D. Kvasnicka, and J. Luitz, *WIEN2k, An Augmented Plane Wave + Local Orbitals Program for Calculating Crystal Properties* (Karlheinz Schwarz, Techn. Universität Wien, Austria, 2001).
[35] E. Sjöstedt, L. Nordström, and D. J. Singh, Solid State Commun. **114**, 15 (2000).
[36] J. P. Perdew, K. Burke, and M. Ernzerhof, Phys. Rev. Lett. **77**, 3865 (1996).
[37] O. Keski-Rahkonen and M. O. Krause, Atom. Data Nucl. Data Tables **14**, 139 (1974).
[38] N. Yabuuchi, Y. Kawamoto, M. Yonemura, T. Ishigaki, A. Hoshikawa, T. Kamiyama, and S. Komaba, in *The 15th International Meeting on Lithium Batteries*, Montreal, Quebec, Canada, Jun. 27–Jul. 3, 2010, p. 618.